Materials Research. 2020; 23(5): e20200205
DOI: https://doi.org/10.1590/1980-5373-MR-2020-0205

1-3 Castor Oil-Based Polyurethane/PZT Piezoelectric Composite as a Possible Candidate for Structural Health Monitoring

*João Gustavo Leite Costa[a], Pedro Henrique Ferrarrezi Rodrigues[a], Leonardo Lataro Paim[c], Alex Otávio Sanches[b], José Antônio Malmonge[a], Michael Jones da Silva[c]**

[a]*Universidade Estadual Paulista (UNESP), Departamento de Física e Química, Ilha Solteira, SP, Brasil*
[b]*Universidade Estadual Paulista (UNESP), Departamento de Engenharia Civil, Ilha Solteira, SP, Brasil*
[c]*Universidade Estadual Paulista (UNESP), Grupo de Materiais Inteligentes e Aplicações, Rosana, SP, Brasil*

Received: May 11, 2020; Revised: August 21, 2020; Accepted: September 26, 2020

In this study, we obtained and characterized a piezoelectric composite with 1-3 connectivity from castor oil polyurethane (PUR) and lead zirconate titanate (PZT) rods. Two samples were obtained, one with 15% PZT volume and the other with 34% PZT volume. The ac electrical properties of the 1-3 piezoelectric composite samples demonstrated the frequency-dependence behavior of disordered solids. The piezoelectric coefficient (d_{33}) was greatly influenced by the number of PZT rods and the matrix curing process. The sample with 34% PZT volume showed a higher d_{33} value, (246 pC/N measured after 30 d of polarization). The composites were evaluated for use in acoustic emission wave sensors for application in structural health monitoring.

Keywords: *Piezoelectric composite, Castor oil polyurethane, PZT, Sensor.*

1. Introduction

Piezoelectricity is simply the conversion of mechanical energy into electrical energy or the reverse process[1]. In piezoelectricity, the generation of electric charges by a material is proportional to the applied mechanical stress, conversely, the change in the physical dimensions of the material is related to the applied electric field[2]. This property has been observed in various materials, e.g., ceramic materials such as lead zirconate titanate (PZT)[3] and barium titanate (BaTiO3)[4], oxides and nitride materials such as zinc oxide (ZnO)[5] and gallium nitride (GaN)[6], and polymeric materials such as poly(vinylidene fluoride) (PVDF)[7,8].

Among all piezoelectric materials, piezoelectric ceramics with a perovskite-type structure such as PZT[9] stand out the most. Even though piezoelectric ceramics have high piezoelectric activity and a high dielectric constant, their mechanical resistance is low. To solve this problem, the piezoelectric ceramic particles have been incorporated into the polymeric matrices to combine the properties of each phase, i.e., the excellent mechanical properties, lightness, and flexibility of the polymeric matrix with the high piezoelectric activity and high dielectric constant of the piezoelectric ceramics[10,11].

The most widely studied polymer/ceramic composites are those with 0-3 connectivity owing to their easy synthesis process. However, for every composite, there are ten possible connectivity patterns[12,13]. In composites with 0-3 connectivity, the ceramic particles are dispersed in the matrix so that there is no contact between the ceramic grains. On the other hand, the polymer phase is connected in three-directions. In this type of composite (with 0-3 connectivity), the polarization of the ceramic particles incorporated in the matrix is not as efficient. This is because the polymer has a low dielectric constant causing a low internal electric field on the ceramic particles[14]. Research in this area has proposed alternatives to increase the electric field on the ceramic particles incorporated in the composite. One of the alternatives is the incorporation of a third conductive phase, such as conductive particles and polymers[15,16].

Another possibility has been to obtain composites with another type of connectivity, such as 1-3[17-19]. In this type of composite, the ceramic particles are connected in one of the three directions, while the polymer phase is self-connected in three directions. In the 1-3 composites, the piezoelectric ceramic acts as an active medium in the conversion of mechanical to electrical energy. On the other hand, the polymer matrix acts as a passive medium, i.e., it transfers mechanical energy between the piezoelectric ceramic and the environment with which the compound interacts[20]. In the 1-3 piezoelectric composite, the polarization of ceramics is more efficient, because the electric field is applied directly on the ceramic and unlike in the 0-3 composite, there is no polymer phase with low dielectric permissiveness between the ceramic grains that limits the electrical field that will be applied.

The combination of a polymeric phase and piezoelectric ceramic rods provides greater electromechanical coupling, less spurious modes, and smaller acoustic impedance[21,22]. In this sense, the application range of 1-3 piezoelectric composites is wide, e.g., transducers for medical ultrasound[23], sensors[24,25], and harvesting energy[26]. There are numerous studies on the production and properties of polymer/ceramic composites with 1-3 connectivity[27-33]. However, there is still much to be explored, mainly from the perspective of the influence of the matrix on the final properties of these

*e-mail: michael.silva@unesp.br

composites. Although the matrix is often seen only as a passive component in 1-3 piezoelectric composites during the transfer of mechanical energy to the ceramic columns, it plays an important role in the reduction of lateral stresses, allowing for greater performance of the ceramic in its thickness direction[31]. As exhibited by 1-3 cementitious-matrix composites, constrictive or microstructural alteration of the matrix on a time scale can bring instability to piezoelectric coefficient (d_{33}) over time, or even improve its constriction and/or densification behaviour[34-37]. This finding can be substantiated if the matrices were to be investigated from the perspective of polymeric matrices that undergo slower curing processes. An investigation is yet to be carried out, even in specialized studies.

Consequently, we outline here an innovative way of obtaining a low-cost 1-3 piezoelectric composite using castor oil-based polyurethane (PUR)/PZT. We illustrate the influence of the constrictive behavior of the matrix on the piezoelectric coefficient of composites with different volume fractions of ceramic. The dielectric, electric, and piezoelectric properties of the composite were analyzed to evaluate its possible application in structural health monitoring sensors.

2. Experimental

2.1 Materials

The prepolymer and polyol components used to obtain castor oil-based polyurethane were obtained from the Analytical Chemistry and Polymer Technology Group of the Institute of Chemistry at the University of São Paulo, campus São Carlos - SP. The stoichiometric ratio of prepolymer/polyol for the preparation of the composite was 1.0/0.7 (1.5 g of the prepolymer and 1.05 g of polyol).

The PZT was purchased from American Piezo Ceramics-APC in powder form (material reference code: 851). Its main characteristics are listed below:

- d_{33} Piezoelectric coefficient ≈ 400 pC/N;
- g_{33} *Piezoelectric voltage constant* ≈ 24×10^{-3} Vm/N;
- Relative dielectric constant at 1 kHz ≈ 1950;
- ρ ≈ 7.6 g/cm^3.

2.2 Obtaining of PZT rods

The PZT rods were obtained by mixing the PZT ceramic particles and water in an agate mortar until the mixture exhibited a pasty appearance. The mixture was then placed in a plastic syringe and extruded to obtain PZT rods. The PZT rods were then dried in an oven at 80 °C and then calcined and sintered at a temperature of 1470 °C (heating rate of 10 °C/min) in a muffle furnace for 1 h. At the end of the process, the samples were washed with acetone in an ultrasonic bath and dried again at 100 °C for 24 h and stored for later use.

2.3 1-3 Piezoelectric composite fabrication

To prepare the composite with 1-3 connectivity, PUR was used as the polymer matrix in a pre-polymer/polyol stoichiometric ratio of 1.0/0.7. To prepare the piezoelectric composites, a teflon mold with a base of uniformly spaced small holes (90 holes) was used to enable the PZT rods remain in a vertical position. Figure 1 illustrates the mold obtained from the 1-3 composite.

Two samples were obtained with a different number of PZT rods, i.e., 90 (filled mold) and 45 (half mold). First, the rods were vertically positioned on mold. After placing the desired number of rods, the solution containing PUR was poured into the mold and remained in the desiccator for 48 h for polymerization and curing of the matrix to take place. After 48 h the samples were sanded to obtain an even surface and then the electrodes were painted with conductive paint. The volumetric fraction of the sample with 90 rods was 66/34 (PUR/PZT), and for the sample with 45 rods, the volumetric fraction was 85/15 (PUR/PZT). All calculations of the volumetric fraction were performed after curing and polymerization of the PUR.

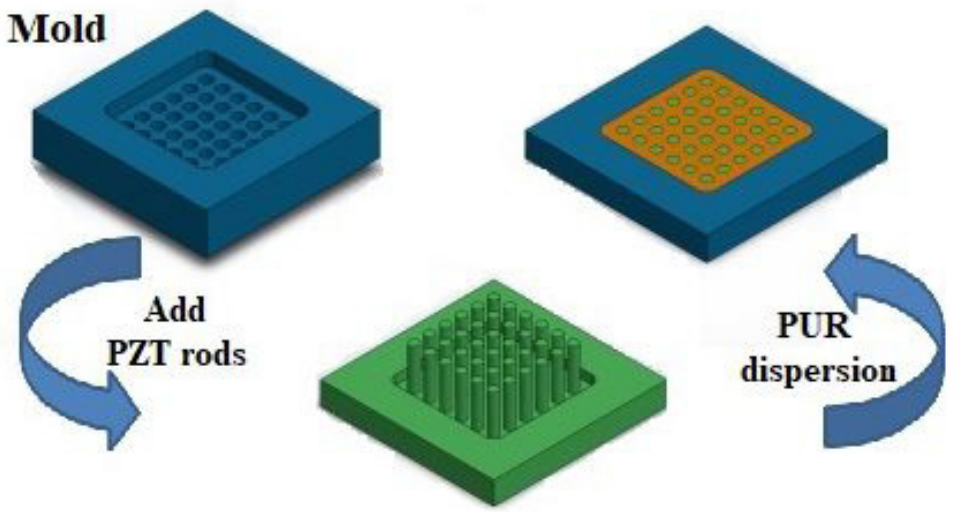

Figure 1. Representation of the teflon mold for obtaining piezoelectric composites with 1-3 connectivity.

2.4 Methods

2.4.1 Impedance and piezoelectric analysis

The dielectric and electrical properties of 1-3 PUR/PZT piezoelectric composites were determined in the frequency range of 10^{-2} – 10^{6} Hz at room temperature, using an SI 1260 Solartron Impedance Analyses with a 1296 Dielectric Interface.

The samples were polarized by applying a constant electric field (1.0 MV/m), using a Trek Model 610 C voltage source. The polarizations were carried out at a temperature of 100 °C for 60 min and cooled to room temperature with the electric field applied. The piezoelectric coefficient, d_{33}, was measured by the American Piezo Ceramics (APC) d_{33} Piezo Tester, model 8000. All measurements were performed at 10 different points, on both metalized sides of each sample. The average d_{33} of each face together with the respective deviation are presented

2.4.2 Tests of structural health monitoring by acoustic emission

To perform the acoustic emission (AE) tests, the 1-3 piezoelectric composite samples were glued on a carbon fiber plate surface (Figure 2) with dimensions of 300 x 300 x 1 mm. Figure 2 shows the experimental setup. An oscilloscope (Agilent DSO6012A) was used to register the sample signals. Two AE simulation methods were used: (i) fall of a metallic sphere, where a metallic sphere of mass 21.4 g was released from a fixed height (5 cm), varying between 5 and 25 cm from the sensor with 5 cm increments[38]. (ii) The well-known Hsu-Nielsen method (ASTM E976-10 standard)[39,40], in which a pencil-lead was broken on the carbon fiber plate at a distance of 15 cm from the sensor.

2.4.3 Morphological analysis

The morphology of the PZT rods was analyzed via scanning electron microscopy (SEM), (EVO LS15, Zeiss, Germany). The samples were fractured and then covered with a thin layer of carbon by the sputtering method.

3. Results and Discussion

3.1 Morphological analysis

Figures 3a and 3b shows the SEM micro images of the PZT rods. The rods clearly had a compact morphology, which was attributed to the joining of the grains in the sintering process. Figure 3b shows an enlargement of one

Figure 2. The perspective view of the testing system of sensors based on 1-3 PUR/PZT piezoelectric composite.

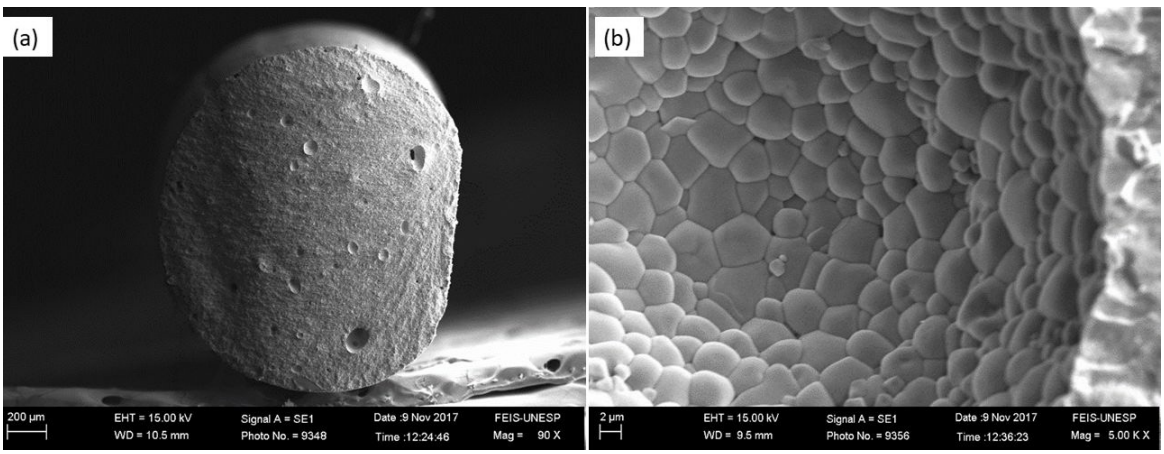

Figure 3. Morphological analysis of PZT rods after calcination and sintering.

of the possible pores. The hexagonal structure obtained from the growth and junction process of the PZT grains can be seen. The distinct morphology observed in the pore region may be attributed to the probable accumulation of water in the region, which reduced the local temperature during the sintering process. On the other hand, as can be seen from the analysis of several samples, the presence of pores is possible and is mainly attributed to the simplified extrusion process adopted. Su et al.[41] observed the similar characteristics for the microstructure of PZT micro-pillars, i.e., dense with small pores in the microstructure after sintering.

3.2 Dielectric and electric properties

The ac electrical response at room temperature of 1-3 PU/PZT composites is showed in Figure 4a and 4b. A strong frequency-dependence on *Z'* and *Z''* for both 1-3 composite samples and neat PUR is observed. As seen in Figure 4a, the samples with a lower number of rods exhibited a higher *Z'* value. The extra insulating character of these samples is attributed to the polymeric matrix. On the other hand, it can be observed that an increase in the volumetric fraction of the rods decreases the *Z'* value. This can be attributed to the sample with 34 vol.% becoming more conducting due to an increase of spatial charge inside the composite.

Figures 5a and 5b show the real (σ′) and imaginary (σ″) part of the ac complex conductivity as a function of frequency at room temperature, respectively, for the 1-3 piezoelectric composite with different amounts of PZT rods and neat PUR. The complex conductivity was obtained from the following equations:

$$\sigma^* = \sigma' + i\sigma'' = \frac{l}{AZ^*} = \frac{L \cdot Z'}{A \cdot \left(Z'^2 + Z''^2\right)} + i\frac{L \cdot Z''}{A \cdot \left(Z'^2 + Z''^2\right)} \quad (1);$$

or

$$\sigma' = \frac{L \cdot Z'}{A \cdot \left(Z'^2 + Z''^2\right)} \quad (2)$$

and

$$\sigma'' = \frac{L \cdot Z''}{A \cdot \left(Z'^2 + Z''^2\right)} \quad (3)$$

where *A* and *L* are the metalized area and thickness of the samples, respectively. Equations 2 and 3 show that σ› is

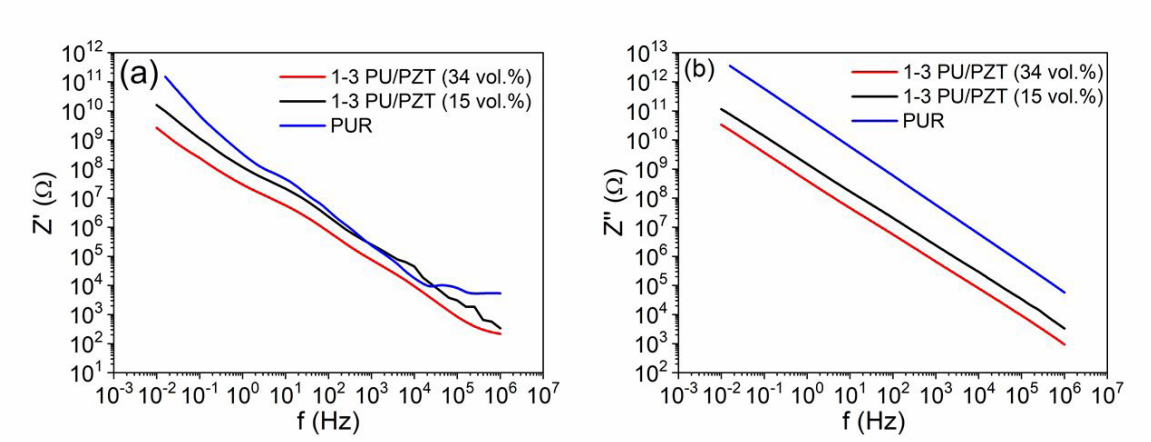

Figure 4. Impedance analysis of neat PUR and 1-3 PUR/PZT piezoelectric composite with different volumetric fraction of PZT rods. (a) real and (b) imaginary part of the impedance complex as a function of frequency at room temperature.

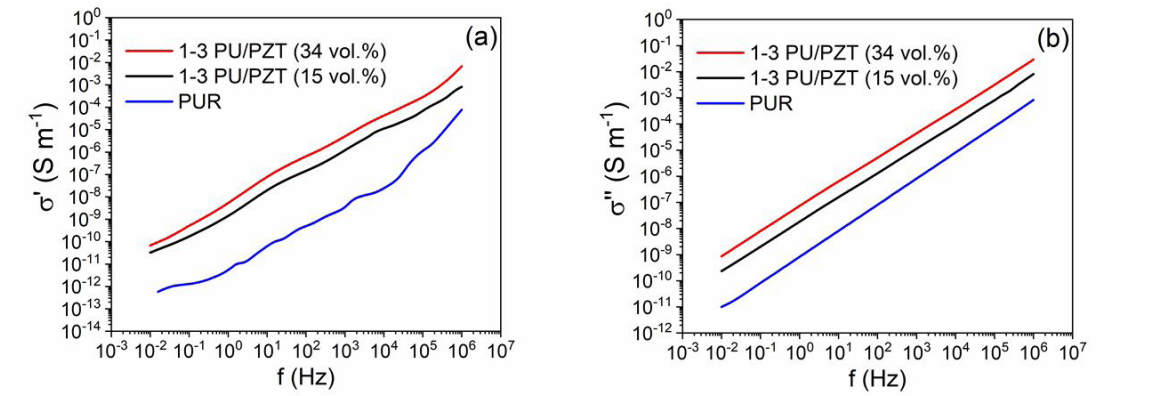

Figure 5. Ac conductivity of the neat PUR and 1-3 PUR/PZT piezoelectric composite with different volumetric fraction of PZT rods. (a) real and (b) imaginary part of the electrical conductivity as a function of frequency at room temperature.

inversely proportional to Z' and σ″ is inversely proportional to Z'', so that as one quantity increases the other decreases. Notably, there is a strong frequency-dependence of σ′ and σ″; both increase as a function of the frequency of the applied electric field. Such behavior is attributed to space charges and electrical dipole movement in the bulk samples[42,43].

A dielectric material, when exposed to an external electric field is subject to the polarization effect, where the charge centers move according to their polarity. The ability of a material to be polarized is represented by a quantity called relative dielectric permittivity (ε_r) which is the measure of the polarizability of material through an applied electric field and relates to its ability to store energy. It can be seen in Figure 6a that the sample with the highest amount of PZT rods (34 vol.%) has greater ε_r value than the sample with 15 vol.% and neat PUR. This behavior is due to the higher dielectric constant of PZT compared to PUR and also to the configuration of the composite. It can be observed that the ε_r value is higher at lower frequencies and decreases with an increase in frequency, i.e. exhibiting a frequency-dependent behavior.

Table 1 shows the relative permittivity values for all samples at approximately 1 kHz. All samples of the piezoelectric composite showed lower ε_r values than neat PZT, as was expected.

While ε_r represents the measurement of the material polarizability caused by an electric field, the capacitance module (C) represents the ability or capacity of a system to store energy. This capacitance is shown in Figure 6b for all samples studied as a function of the frequency at room temperature. The 1-3 PUR/PZT composite with 34 vol.% showed a capacitance value of approximately three orders of greatness greater than neat PUR. This is attributed to the greater dipolar polarization of the ferroelectric domains of the PZT in the composites[16].

3.3 Longitudinal piezoelectric coefficient d_{33}

Samples of the 1-3 PUR/PZT piezoelectric composite with 15 and 34 vol.% were polarized under an electric field of 1.0 MV/m for 60 min at temperatures of 100 °C. To verify the stability of the polarization, d_{33} measurements were taken after 1 d and 30 d of polarization. To verify the uniformity of the d_{33} measurements were also taken according to the metalized faces of the composites and the results shown in Figure 7. Average uniformity can be observed in terms of the d_{33} values of the samples. The variation found is correlated to both the connectivity of the composites and the specific measurement methodology. As expected, the sample with 34 vol.% showed a higher d_{33} than the sample with 15 vol.%.

The sample with 15 vol.%, exhibited a higher piezoelectric coefficient d_{33} after 30 d. This type of behavior is generally observed in matrices with constrictive behavior and reduced porosity from aging, such as cement[34-37]. The constrictive behavior of cementitious matrices, together with unstable dipoles (organized during the ionic polarization process) tends to cause instability of the piezoelectric coefficient in the initial post-polarization periods. As such, their stability for long post-polarization periods can only be estimated[37]. The d_{33} variation observed in the sample with 15 vol.% (45 rods) may be attributed to the longer curing time of PUR as reported by Alves et al.[44] Over time, the polymer matrix becomes more compact due to the rearrangement and contraction of the polymer chains, which in turn compresses the ceramic rods, improving d_{33} after 30 d. This behavior is hardly observable in the sample with 34 vol.% (90 rods), which has the lowest polymeric fraction of the matrix.

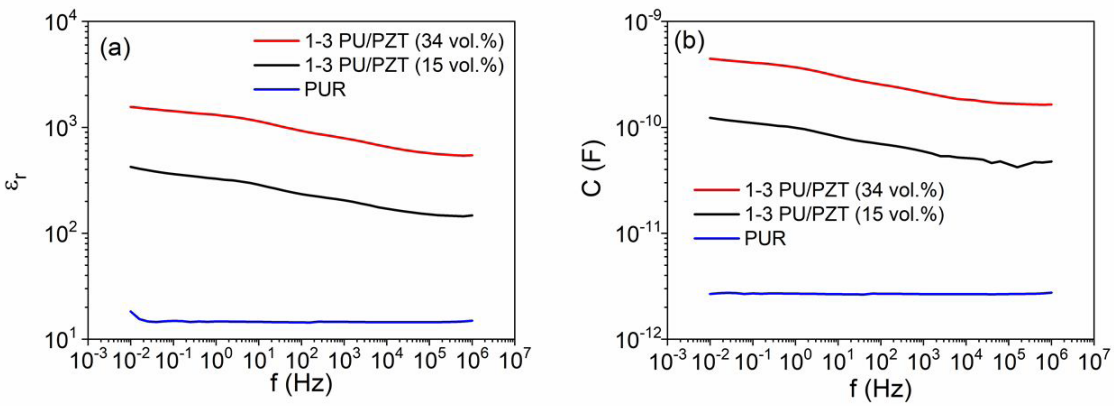

Figure 6. Evaluation of the (a) relative permittivity and (b) capacitance as a function of frequency at room temperature for the samples of the 1-3 piezoelectric composite and for the neat PUR.

Table 1. ε_r value of the samples of 1-3 PUR/PZT composites, neat PUR and PZT at 1 kHz.

Samples	PUR	PZT	PUR/PZT 34 vol.% (90 rods)	PUR/PZT 15 vol.% (45 rods)
ε_r	14	1950	789	215

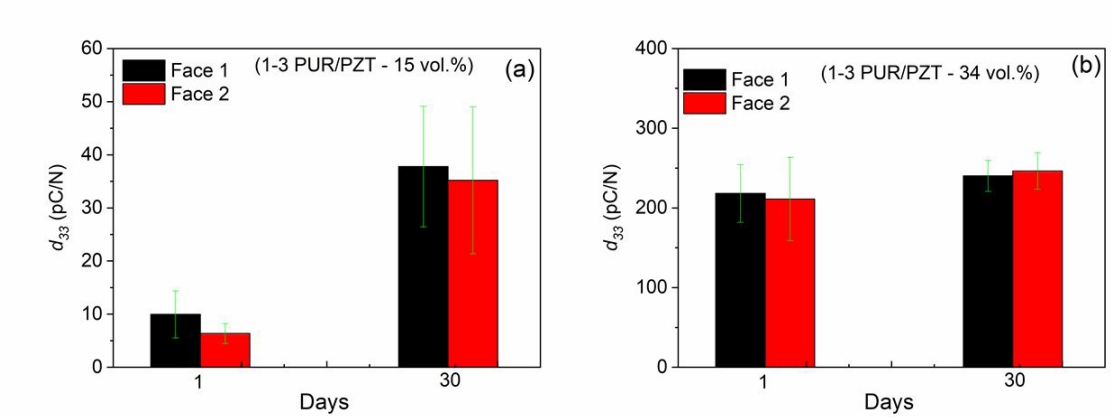

Figure 7. d_{33} values obtained for 1-3 PUR/PZT composite samples with 15 vol.% (45 rods) and 34 vol.% (90 rods) of PZT. Measurements carried out one and 30 d after polarization. The face 1 and face 2 refers to the face of the sample that was subjected to the positive and negative pole of the polarization source, respectively.

Table 2. Comparative analysis of the d_{33} value of the 1-3 PUR/PZT 1-3 composite samples and works in the literature.

Samples	d_{33} (pC/N)	References
PZT	400	Manufacturer's data
PUR/PZT 1-3, 34 vol.% (90 rods)	246	This work
PUR/PZT 1-3, 15 vol.% (45 rods)	37	This work
1-3 Epoxy/PZT–PMS–PZN	300	Gu et al.[45]
1-3 Epoxy/BNKT–ST	104	Li and Zuo[46]
1-3 Araldite-F/PZT	260	Mishra et al.[47]

The results found in this work are within the range of values found in previous studies (Table 2)[45-47]. Table 2 shows the d_{33} values of the 1-3 PUR/PZT composite and previous related studies for comparison.

3.4 Sensor testing

Structural health monitoring (SHM) methods are used for the detection, evaluation, and characterization of an engineering structure over time using a sensor. The non-destructive techniques (NDA), such as acoustic emission (AE)[48] are the most popular when it comes to evaluation. AE, through sensors arranged on the surface or in situ in a given material that extract information about the nature of the emission source[48], is used to measure and store elastic wave information generated by a rapid release of energy when a sudden deformation occurs in the material

Figure 8 shows the response of the sensors of 1-3 composites (a) with 15 and (b) 34 vol.% for the fall of the metallic sphere from a height of 5 cm. The distance of the 1-3 composites from the sensor was 5 cm. As expected, it is observed that the 1-3 composite with 34 vol.% generated a greater signal than the sample with 15 vol.% (2.3 V for a sample with 34 vol.% and 0.18 V for a sample with 15 vol.%). This behavior corroborates with the tests of the piezoelectric coefficient d_{33}, in which the sample with 34 vol.% exhibited a higher d_{33} than the sample with 15 vol.%.

By fixing the release height of the sphere at 5 cm it was possible to evaluate the sensitivity of the sensor response as a function of the distance from the AE simulation source. As can be seen from Figure 9a and 9b, the sensor response decreases as the impact distance increases. For the distance of 20 cm, the voltage drops to approximately 50% for both sensors, but they still maintaining a good electrical response.

The Hsu-Nielsen method (pencil-lead break) was carried out only with the 34 vol.% sample because the sample with 15 vol.% did not show satisfactory signal strength. Figure 10a shows the response as a function of time for the pencil-lead break test. It was possible to observe a good response through the sensor with an amplitude of 0.17 V without amplification or filtering (at 15 cm distance between the simulator source and the sensor).

The sensor response was also analyzed as a function of the distance between the pencil-lead break and the sensor, as shown in Figure 10b. It was observed that the signal of the sensor response decreased in the same way as the ball drop test. This is attributed to the attenuation of the elastic waves. However, the sensor still showed sensitivity even for greater distances where the signal was collected with no amplification.

Obtaining piezoelectric composites from a bio-based polymer matrix is always difficult. PUR, in its natural form, is oil. When obtaining it in film form, many bubbles appear that can damage the response of the sensor and electromechanical coupling. In this sense, the methodology of obtaining PUR should follow a controlled procedure with low humidity and the water-free surface utilized (both the surface of the PZT rods and the samples mold). We observed

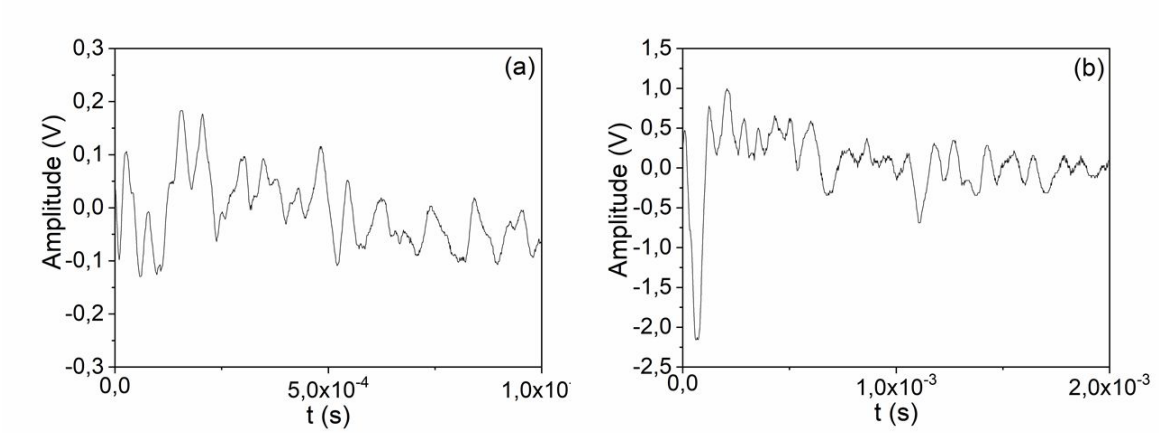

Figure 8. Sensor response to the massive ball drop as a function of the time for (a) 1-3 PUR/PZT sample with 15 vol.% (45 rods) and (b) 34 vol.% (90 rods) of PZT.

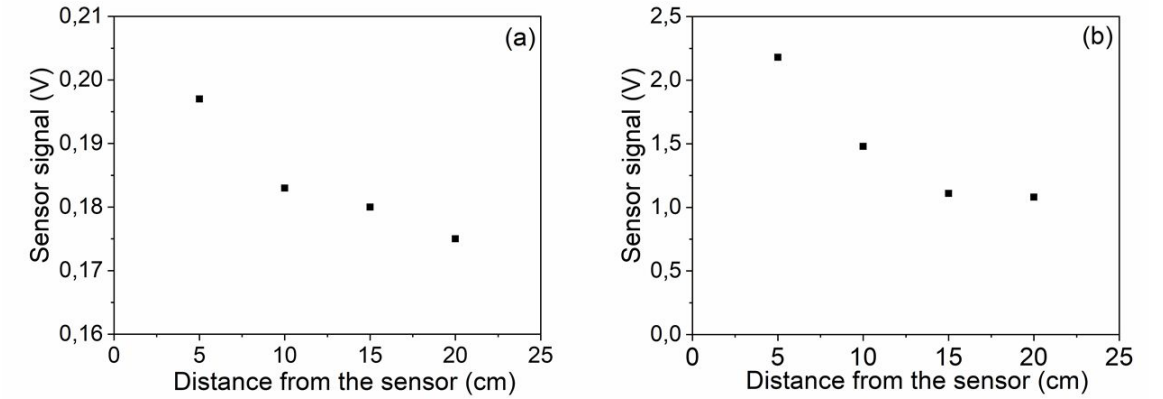

Figure 9. Sensor response to the massive ball drop for different distances from the AE source. (a) 1-3 PUR/PZT sample with 15 vol.% (45 rods) and (b) 34 vol.% (90 rods) of PZT.

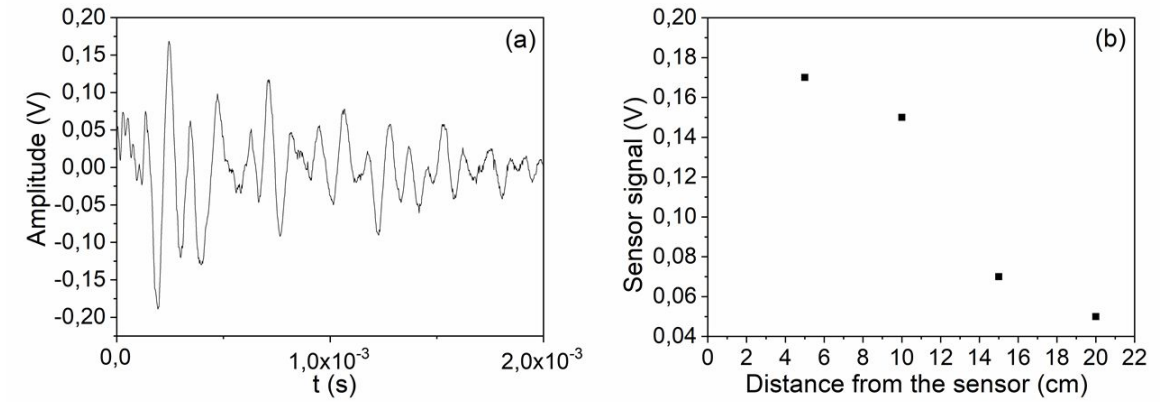

Figure 10. Sensor response to a pencil-lead break as a function of the time for sample with 34 vol.% (90 rods) of PZT.

that controlling the number of bubbles in the process of obtaining the 1-3 piezoelectric composite can improve its final dielectric and piezoelectric properties.

Other methodologies can also be used to improve the sensor response and sensor electromechanical coupling, mainly aimed at the structure of the PZT rods and composite[49-51]. A study conducted by Cheng et al.[49] evaluated adjusting the piezoelectric ceramic volume fraction and shape parameters for a 1-3 piezoelectric ceramic – cement composite. The authors demonstrated that the adjustment of the structures of the composite improved its sensitivity in structural health monitoring[49].

Directly embedding the piezoelectric sensor into structures that monitor the performance and detect the damage is an alternative methodology to improve the sensor response[50,51]. Ma et al.[50] investigated the behavior of a cement-based 1−3 piezoelectric composite sensor embedded into structures and the results showed that both sensors had good accuracy, linearity, and frequency bandwidth.

4. Conclusion

Piezoelectric composites with 1-3 connectivity obtained from castor oil polyurethane and PZT rods were successfully developed using the align-and-fill method. Two samples containing 15 and 34 vol.% of PZT rods were prepared. Dielectric spectroscopy was performed using the impedance spectroscopy technique in the frequency range of $10^{-2} – 10^{6}$ Hz. The composites showed a much higher dielectric constant than neat PUR in the entire frequency range. This is attributed to the high value of the PZT dielectric constant and the configuration of the composite. The piezoelectric coefficient d_{33} values were approximately 37 and 246 pC/N for the composite with a volume ratio of 15 vol.% (45 rods) and 34 vol% (90 rods), respectively. The sensors were surface-mounted on a carbon fiber plate and the fall of a metallic sphere and pencil-lead break were used as acoustic emission sources. The sample with 34 vol.% showed the best results. It thus qualified as a possible candidate for a sensor of AE waves.

5. Acknowledgments

The authors acknowledge the São Paulo Research Foundation (FAPESP), grant 2016/15718-2 and 2017/19809-5, for their financial support.

6. References

1. Lee BY, Zhang J, Zueger C, Chung W-J, Yoo SY, Wang E, et al. Virus-based piezoelectric energy generation. Nat Nanotechnol. 2012;7(6):351-6.
2. Gallego-Juarez JA. Piezoelectric ceramics and ultrasonic transducers. J Phys E Sci Instrum. 1989;22(10):804-16.
3. Tian G, Deng W, Gao Y, Xiong D, Yan C, He X, et al. Rich lamellar crystal baklava-structured PZT/PVDF piezoelectric sensor toward individual table tennis training. Nano Energy. 2019;59:574-81.
4. Mei T, Dai Q, Zheng W, Chen T. Strain properties and piezoelectric constant of lead-free barium titanate ceramics. Mater Res Express. 2019;6(10):106301.
5. Loh KJ, Chang D. Zinc oxide nanoparticle-polymeric thin films for dynamic strain sensing. J Mater Sci. 2011;46(1):228-37.
6. Lueng CM, Chan HLW, Surya C, Choy CL. Piezoelectric coefficient of aluminum nitride and gallium nitride. J Appl Phys. 2000;88(9):5360-3.
7. Zhang Y, Xie M, Roscow J, Bao Y, Zhou K, Zhang D, et al. Enhanced pyroelectric and piezoelectric properties of PZT with aligned porosity for energy harvesting applications. J Mater Chem A Mater Energy Sustain. 2017;5(14):6569-80.
8. Das-Gupta DK. Pyroelectricity in polymers. Ferroelectrics. 1991;118(1):165-89.
9. Heywang W, Lubitz K, Wersing W, editors. Piezoelectricity: evolution and future of a technology. New York: Springer Science & Business Media; 2008.
10. Ioannou G, Patsidis A, Psarras GC. Dielectric and functional properties of polymer matrix/ZnO/BaTiO3 hybrid composites. Compos, Part A Appl Sci Manuf. 2011;42(1):104-10.
11. Salaeh S, Muensit N, Bomlai P, Nakason C. Ceramic/natural rubber composites: influence types of rubber and ceramic materials on curing, mechanical, morphological, and dielectric properties. J Mater Sci. 2011;46(6):1723-31.
12. Jain A, Prashanth KJ, Sharma AK, Jain A, P.N R. Dielectric and piezoelectric properties of PVDF/PZT composites: a review. Polym Eng Sci. 2015;55(7):1589-616.
13. Sampathkumar P, Gowdhaman P, Sundaram S, Annamalai V. A review on PZT-polymer composites: dielectric and piezoelectric properties. Nano Vision. 2013;3(3):223-30.
14. Liu XF, Xiong CX, Sun HJ, Dong L, li R, Liu Y. Piezoelectric and dielectric properties of PZT/PVC and graphite doped with PZT/PVC composites. Mater Sci Eng B. 2006;127(2-3):261-6.
15. Sanches AO, Kanda DHF, Malmonge LF, da Silva MJ, Sakamoto WK, Malmonge JA. Synergistic effects on polyurethane/lead zirconate titanate/carbon black three-phase composites. Polym Test. 2017;60:253-9.
16. Campos Fuzari G Jr, Orlandi MO, Longo E, Melo WLB, Sakamoto WK. Effect of controlled conductivity on thermal sensing property of 0–3 pyroelectric composite. Smart Mater Struct. 2013;22(2):025015.
17. Shindo Y, Narita F, Watanabe T. Nonlinear electromechanical fields and localized polarization switching of 1-3 piezoelectric/polymer composites. Eur J Mech A, Solids. 2010;29(4):647-53.
18. Lin CH, Muliana A. Micromechanics modeling of hysteretic responses of piezoelectric composites. In: Guedes RM, editor. Creep and fatigue in polymer matrix composites. Oxford: Woodhead Publishing; 2019. p. 121-55.
19. Sun R, Wang L, Zhang Y, Zhong C. Characterization of 1-3 Piezoelectric Composite with a 3-Tier Polymer Structure. Materials. 2020;13(2):397.
20. Sakthivel M, Arockiarajan AA. An effective matrix poling characteristics of 1-3-2 piezoelectric composites. Sens Actuators A Phys. 2011;167(1):34-43.
21. Wang C, Zhang R, Jing Y, Cao W. The effect of polymeric filler on poling behavior and thermal stability of 1-3 piezoelectric composites. J Phys D Appl Phys. 2016;49(2):025301.
22. Lee HJ, Zhang S. Design of low-loss 1-3 piezoelectric composites for high-power transducer applications. IEEE Trans Ultrason Ferroelectr Freq Control. 2012;59(9):1969-75.
23. Wu Z, Xi K. Characterization of PMN–PT piezoelectric single crystal and PMN–PT 1–3 composite at elevated temperatures by electrical impedance resonance analysis. Ultrasonics. 2011;54(5):1318-22.
24. Zhang J, Lu Y, Lu Z, Liu C, Sun G, Li Z. A new smart traffic monitoring method using embedded cement-based piezoelectric sensors. Smart Mater Struct. 2015;24(2):025023.
25. Makireddi S, Balasubramaniam KA. 1–3 piezoelectric fiber reinforced carbon nanotube composite sensor for crack monitoring. J Inst Eng India Ser C. 2016;97(3):345-56.
26. Stuber VL, Deutz DB, Bennett J, Cannel D, de Leeuw DM, van der Zwaag S, et al. Flexible lead-free piezoelectric composite materials for energy harvesting applications. Energy Technol. 2019;7(1):177-85.
27. Li X, Wang L, Zhong C, Zhang Y. The effect of piezoelectric ceramic volume fraction on the thickness vibration characteristics of 1-3 piezocomposites. Ferroelectrics. 2018;531(1):84-91.
28. Avellaneda M, Swart PJ. Calculating the performance of 1–3 piezoelectric composites for hydrophone applications: an effective medium approach. J Acoust Soc Am. 1998;103(3):1449-67.
29. Abrar A, Zhang D, Su B, Button TW, Kirk KJ, Cochran S. 1–3 connectivity piezoelectric ceramic–polymer composite transducers made with viscous polymer processing for high frequency ultrasound. Ultrasonics. 2004;42(1-9):479-84.
30. Mi X, Qin L, Liao Q, Wang L. Electromechanical coupling coefficient and acoustic impedance of 1-1-3 piezoelectric composites. Ceram Int. 2017;43(9):7374-7.

31. Yang Z, Wang H, Zeng D, Zhao C, Chen Z. Dynamic modeling of 1–3 piezoelectric composite hydrophone and its experimental validation. Compos Struct. 2016;150:246-54.
32. Zhang Y, Wang L, Qin L. Equivalent parameter model of 1-3 piezocomposite with a sandwich polymer. Results in Physics. 2018;9:1256-61.
33. He C, Wang Y, Lu Y, Liu Y, Wu B. Design and fabrication of air-based 1-3 piezoelectric composite transducer for air-coupled ultrasonic applications. J Sens. 2016;2016:4982616.
34. Li Z, Dong B, Zhang D. Influence of polarization on properties of 0–3 cement-based PZT composites. Cement Concr Compos. 2005;27(1):27-32.
35. Wang F, Wang H, Song Y, Sun H. High piezoelectricity 0–3 cement-based piezoelectric composites. Mater Lett. 2012;76:208-10.
36. Pan HH, Lin DH, Yang RH. High piezoelectric and dielectric properties of 0–3 PZT/cement composites by temperature treatment. Cement Concr Compos. 2016;72:1-8.
37. Santos JA, Sanches AO, Akasaki JL, Tashima MM, Longo E, Malmonge JA. Influence of PZT insertion on Portland cement curing process and piezoelectric properties of 0–3 cement-based composites by impedance spectroscopy. Constr Build Mater. 2020;238:117675.
38. Sanches AO, Teixeira GF, Zaghete MA, Longo E, Malmonge JA, Silva MJ, et al. Influence of polymer insertion on the dielectric, piezoelectric and acoustic properties of 1-0-3 polyurethane/cement-based piezo composite. Mater Res Bull. 2019;119:110541.
39. Freitas RLB, Sakamoto WK, Freitas LPS, Castro F, Lima Filho AP, Kitano C, et al. Characterization of PZT/PVDF composite film as functional material. IEEE Sens J. 2018;18(12):5067-72.
40. Wenger MP, Blanas P, Shuford RJ, Das-Gupta DK. Characterization and evaluation of piezoelectric composite bimorphs for in-situ acoustic emission sensors. Polym Eng Sci. 1999;39(3):508-18.
41. Su B, Zhang D, Button TW. Embossing of ceramic micro-pillar arrays. J Eur Ceram Soc. 2012;32(12):3345-9.
42. Rebeque PV, Silva MJ, Cena CR, Nagashima HN, Malmonge JA, Kanda DHF. Analysis of the electrical conduction in percolative nanocomposites based on castor-oil polyurethane with carbon black and activated carbon nanopowder. Polym Compos. 2019;40(1):7-15.
43. Chiu FC. A review on conduction mechanisms in dielectric films. Adv Mater Sci Eng. 2014;2014:578168.
44. Alves WF, Kanda DH, Malmonge LF, Malmonge JA, Mattoso LH. Preparation and characterization of castor oil-based polyurethane/poly (o-methoxyaniline) blend film. J Appl Polym Sci. 2007;105(2):706-9.
45. Gu X, Yang Y, Chen J, Wang Y. Temperature-dependent properties of a 1-3 connectivity piezoelectric ceramic–polymer composite. Energy Harvesting and Systems. 2015;2(3-4):107-12.
46. Li F, Zuo R. Bismuth sodium titanate based lead-free ceramic/epoxy 1–3 composites: fabrication and electromechanical properties. J Mater Sci Mater Electron. 2014;25(6):2730-6.
47. Mishra S, Unnikrishnan L, Nayak SK, Mohanty S. Advances in piezoelectric polymer composites for energy harvesting applications: a systematic review. Macromol Mater Eng. 2019;304(1):1800463.
48. Li W, Kong Q, Ho SCM, Lim I, Mo YL, Song G. Feasibility study of using smart aggregates as embedded acoustic emission sensors for health monitoring of concrete structures. Smart Mater Struct. 2016;25(11):115031.
49. Cheng X, Xu D, Lu L, Huang S, Jiang M. Performance investigation of 1-3 piezoelectric ceramic–cement composite. Mater Chem Phys. 2010;121(1-2):63-9.
50. Ma Y, Cheng X, Jiang Q, Li Y. A cement-based 1− 3 piezoelectric composite sensor working in d 15 mode for the characterization of shear stress in civil engineering structures. Smart Mater Struct. 2018;27(11):115013.
51. Zhang F, Feng P, Wang T, Chen J. Mechanical-electric response characteristics of 1-3 cement based piezoelectric composite under impact loading. Constr Build Mater. 2019;228:116781.